Detection and location of sub-solar flares and Gamma Ray Burst GRB221009A from GNSS Ionosphere

Manuel Hernández-Pajares[1,2*], David Moreno-Borràs[1,2], Octavi Fors[3], Julien Poyatos[3], Qi Liu[1], Victoria Graffigna[1,2], Germán Olivares-Pulido[1,2], David Roma-Dollase[2], Alberto García-Rigo[2], Enric Monte-Moreno[4], Heng Yang[5,4,1], Haixia Lyu[6,1], José M. Gómez-Cama[9], Javier Ventura-Traveset[7] and Raul Orús-Pérez[8]

[1*]Res. Group UPC-IonSAT, Dept. Mathematics, Universitat Politècnica de Catalunya, Mod. C3 Campus Nord, c/ Jordi Girona 1, Barcelona, 08034, , Spain.
[2]IEEC, Barcelona, Spain.
[3]Dept. de Física Quàntica i Astrofísica, Institut de Ciències del Cosmos (ICCUB), Universitat de Barcelona, IEEC-UB, Martí i Franquès 1, Barcelona, 08028, Spain.
[4]Res. Group UPC-TALP, Dept. Signal Theory and Communications, Universitat Politècnica de Catalunya, Campus Nord, c/ Jordi Girona 1, Barcelona, 08034, Spain.
[5]School of Electronic Information and Engineering, Yangtze Normal University, Chongqing, 408100,, China.
[6]GNSS Research Center, Wuhan University, Wuhan, China.
[7]Centre Spatial de Toulouse, ESA, Toulouse, France.
[8]ESTEC, ESA, Noordwijk, The Netherlands.
[9]Department of Engineering Electronics, Universitat de Barcelona, Barcelona, Spain.

*Corresponding author(s). E-mail(s): manuel.hernandez@upc.edu;
Contributing authors: mbdavid297@gmail.com;
octavifors@icc.ub.edu; julienpoyatos@icc.ub.edu;
qi.liu@henu.edu.cn,q.liu@upc.edu; victoria.graffigna@upc.edu;

german.olivares@upc.edu; roma@ieec.cat;
alberto.garcia.rigo@upc.edu; enric.monte@upc.edu;
h.yang@yznu.edu.cn,h.yang@upc.edu; hxlyu@whu.edu.cn;
jm.gomez@icc.ub.edu; Javier.Ventura-Traveset@esa.int;
raul.orus.perez@esa.int;

Abstract

In time scales of minutes the solar subflares and gamma ray bursts, like GRB221009A, can respectively release, small but close and huge but very far away amounts of electromagnetic energy, in Extreme Ultraviolet (EUV), X-ray and γ- ray, among other bands. However the availability of conventional astronomical sensors for these bands, for instance in EUV, fundamental to characterize the habitability zone of exoplanets in hosting stars, is presently very limited or just non existing. At the same time the satellites of the Global Navigation Satellite Systems (GNSS) are orbiting the Earth, sending multifrequency signals crossing the Ionosphere, openly gathered by thousands of worldwide permanent ground-based receivers. This constitutes an unique sensor of the free electron content distribution, mainly produced by the Sun EUV and X-ray flux. Here we show how the tandem GNSS-Ionosphere is able to detect and locate by the first time the solar subflares and the gamma ray burst sources like GRB221009A, from the overionization footprint, small but very characteristics and well predicted by First-Principles. We found, coinciding with the good blind location of the Sun position, the agreement of the sub-solar event epochs with the ones from direct GOES and direct SOHO-SEM satellite based measurements in X-ray and EUV bands, respectively. And, coinciding with the close blind location of GRB221009A source position, we have found a good agreement of the peak times in the GNSS flux proxies vs. the peak times in direct satellite based measurements in X- and specially γ-ray bands, measured by Solar Orbiter and Fermi satellites, respectively. Our results demonstrate the very high sensitivity of this new concept and new associated technique. We anticipate this work to be a major step for converting GNSS Ionosphere in an unique omnidirectional real-time 24/7 astronomical sensor in EUV, X-ray and γ flux, openly available for new potential findings in Astronomy.

Keywords: Solar sub-flares, gamma ray bursts, GNSS ionosphere, small EUV flux variations

During the last three decades, the Global Navigation Satellite Systems (GNSS) have become a sounder of the Earth ionosphere with unprecedent spatial and temporal resolution, opening a new field, the GNSS Ionosphere ([1]). GNSS is presently disposing of more than 100 Medium Earth Orbiting (MEO) satellites of the GPS, Galileo, Beidou and GLONASS constellations, transmitting multi-frequency L-band signals gathered from thousands of permanent GNSS

receivers and crossing the ionosphere. This is typically distributed from around 50 km to 1000 km height, where some predominant air molecules, such as O_2 and NO at the very bottom and mostly O above, are partially ionized respectively by the X-ray and specially Extreme Ultraviolet (EUV) solar flux, dependence which are the fundamental roots of the new presented technique.

In this way GNSS ionosphere is able to provide a unique spatial and time resolution in the estimated global distribution of ionosphere electron content ([2], [3]), either in real-time [4]. And this is quickly improving existing fields, like precise GNSS positioning [5, 6] and GPS Meteorology [7]. Moreover it opens new applications, like the potential warning of natural hazard events, e.g. tsunamis [8], among becoming a fully astronomical instrument, as we present in this work, by extending the very first research in solar flares [9–11] and potential detection of stellar superflares [12].

In order to consolidate and extend such result, contributing to definitely open a new GNSS Ionosphere-based Astronomy window, we have developed a new GNSS overionization blind model from extraterrestrial sources, the EXtra SOLar sources search based on EUV, gamma or X-ray radiation RAte drift from GNSS (hereinafter EXSOLERAdrift-search), much more sensitive than the previous ones.

Indeed, a first representative example of solar flare and subflare detection is shown in Extended Data Figure 1, corresponding to the time interval of 02h-03h UTC of May 22, 2021 (day 142), which includes a weak (C-class) flare (see top plot in same figure). It can be seen that the p-value validated SOLar source search based on EUV, gamma or X-ray radiation RAte drift (SOLERAdrift) index (green points in central plot) and the distance of the EXSOLERAdrift-search grid center winner to the Sun over the celestial sphere (dark-violet points in the same central plot) agree well between them and, at the same time, vs the direct X-ray and EUV band solar flux measurements, provided respectively by GOES and SOHO-SEM photometers (top and bottom plots in Extended Data Figure 1).

In particular, it can be seen how the C6.2-class flare ionospheric footprint is perfectly detected by multi-GNSS at 1 Hz, including the detail of the double peak only observed in direct EUV flux measurements before 03h UTC. But, also, the previous extremely weak flare that happened around 02.75h UTC (B1.7) is perfectly detected in terms of both p-value validated SOLERAdrift index peak and SOLERAdrift-search distance clearly below 20^{o}, reflected similarly in this case, in the direct solar flux measurements in X-ray and EUV bands.

And regarding the other two extremely weak solar flares with peaks within 02h-03h UTC, which happened around 2.15h UTC, we only see at the beginning and end of the flare, a decrease of the SOLERAdrift-search Sun-distance below 20^{o}, but practically no significant SOLERAdrift value. This fact is compatible with the seemenly flat reference EUV flux in this time interval 2.175-2.2h UTC, at the noise level of the available SOHO-SEM measurement.

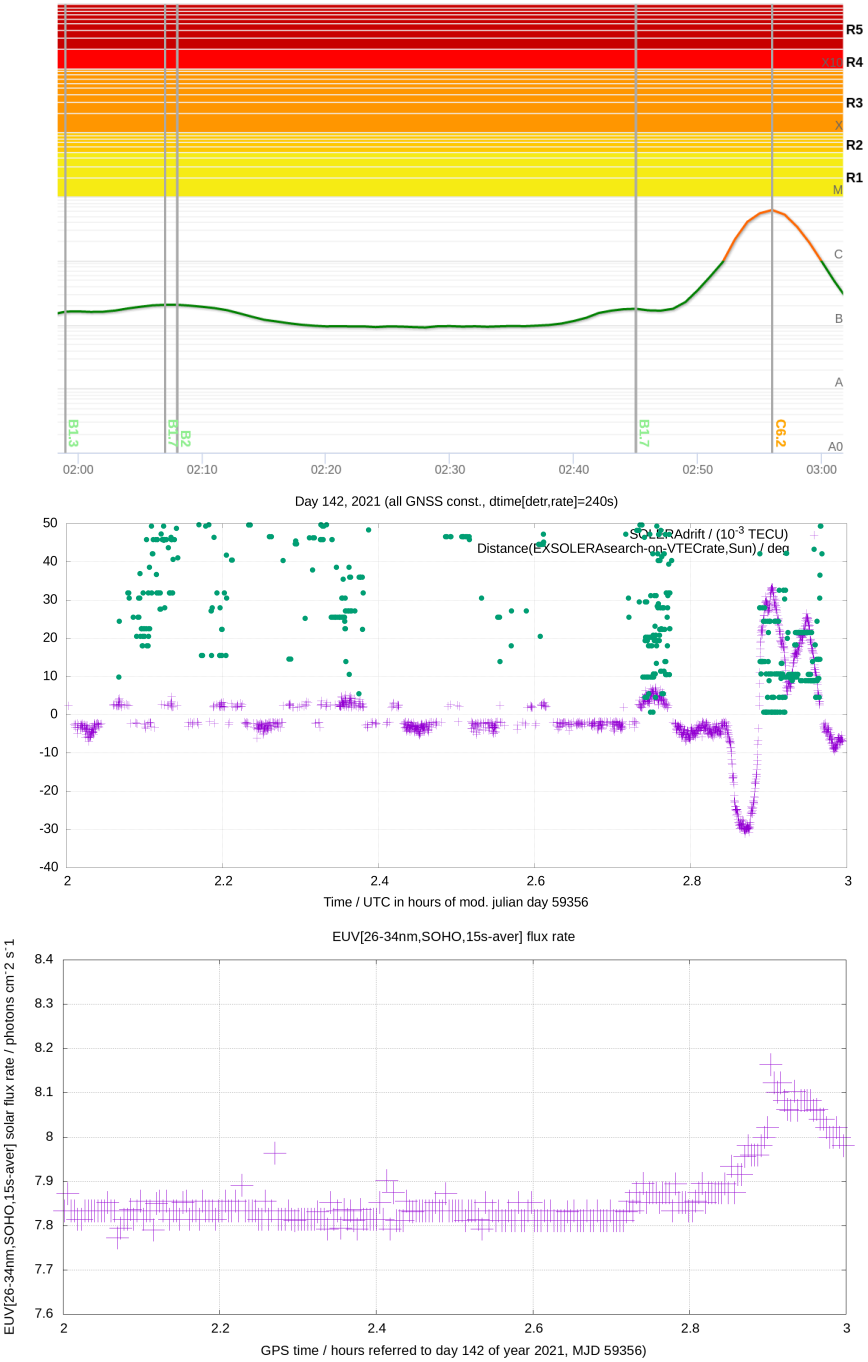

Fig. 1 (Extended Data) Time evolution, since 02h to 03h UTC on day 142 of 2021 of: (1) the directly (GOES) measured solar flux in X-ray band (1-minute solar average in $[1, 8]\mathring{A}$, top plot), (2) the indirectly (ionospheric footprint with GNSS) EUV-flux sensitive SOLERAdrift index and the SOLERAdrift-search distance to the Sun (green and dark-violet points in central plot), and (3) the directly (SOHO-SEM) measured solar EUV flux rate in [26,34]nm window (bottom plot).

The last but not the least in this first representative example: a clear detection is provided by SOLERAdrift-search around 2.37h in both validated SOLERAdrift index and distances to the Sun much less than 20^{o} with SOLERAdrift-search. It is difficult to confirm a counterpart in the direct X-band flux measurements, but in the direct EUV flux measurements a tiny increase appears to be apparent from 2.35h to 2.8h UTC, at the noise limit of the SOHO-SEM flux measurements. This apparent coincidence suggests the possibility that the indirect GNSS-based technique may achieve a higher sensitivity than the available direct EUV measurements ($\lesssim 0.01 \text{x} 10^{9}$ EUV[26-34]nm photons / cm^2 / s).

Next we present the results analyzing a still more challenging scenario, that occurred during the subsequent hour, i.e., 03h-04h UTC: As it can be seen in the top plot of Figure 2, first, an extremely weak B4-class flare around 3.55h, is very clearly detected with GNSS (central plot in Figure 2), in agreement with a small increase of EUV flux directly observed at the bottom plot.

However, secondly, and among such B-class flare, the direct solar X-ray flux measurements show small increases, below the flare level, around 3.65h and 3.85h UTC, also detected in the direct EUV flux measurements at the bottom plot. It can be seen in the central plot of Figure 2 that both are well detected with GNSS. But the GNSS method shows two additional validated flux increases at 3.02h and 3.22h that are in agreement with direct EUV flux measurements, especially the first but also in the second event at the limit of the noise of direct measurements. However, both events are not seen in the direct events in X-ray band flux which is a good example of flux variations that can happen / can be detected, or not, depending on the electromagnetic frequency domain.

Gamma-ray bursts (GRBs) are bright flashes of gamma-rays reaching the Earth. GRBs last typically a ten of seconds, after an initial prompt phase of less than 100 s, and spectral energy peak on the γ-ray band. They are considered the most luminous events in the universe, with an energy content of 10^{51} ergs. The considered source of the GRB energy is the gravitational collapse of matter to form a compact object such as a black hole (Gehrels & P. Meszaros, 2012[13]).

When the new GNSS Ionosphere based astronomical technique is applied during the October 9, 2022 (day 257), with dt=120s=2*60s detrending time and multiGNSS measurements under 30s observation cadence, the maximum of apparent overionization during the whole day is focused within few degrees from GRB221009A location (see Figure 3). And this is coinciding in time as well with the GRB event, around 13h20m UTC (i.e. 48000 seconds of day), the brightest one recorded so far, from the source, presently 2.4 billion-years away. As a consequence GRB221009A produced an ionospheric response indirectly detected by VLF/LF signals (Pal et al. 2023[14]), with much lower frequencies, i.e., much more sensitive, than the the L-band GNSS signals. This makes the indirect GRB detection throught GNSS Ionosphere measurements extremely challenging.

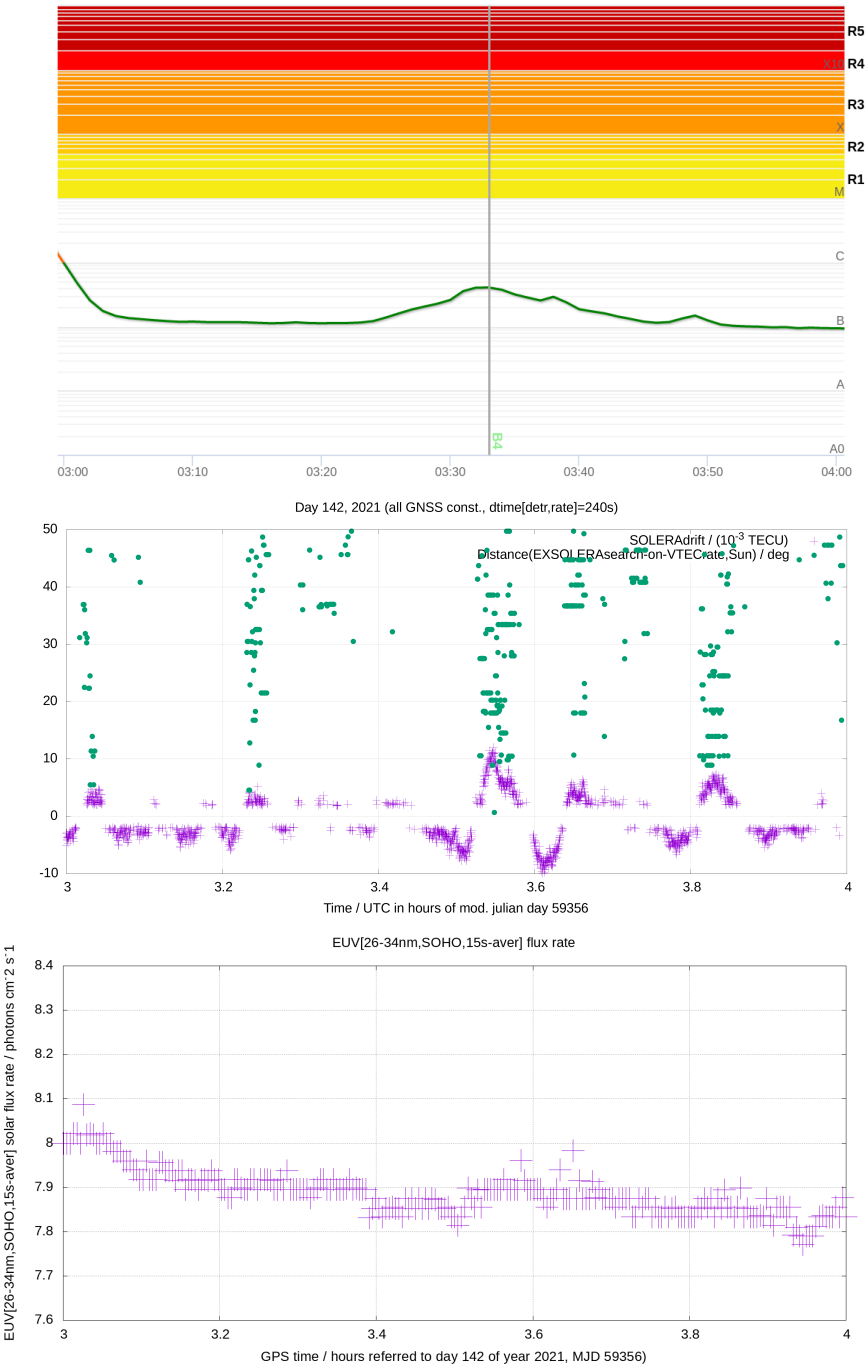

Fig. 2 Time evolution, since 03h to 04h UTC on day 142 of 2021 of: (1) the directly (GOES) measured solar flux in X-ray band (1-minute solar average in $[1,8]\mathring{A}$, top plot), (2) the indirectly (ionospheric footprint with GNSS) EUV-flux sensitive SOLERAdrift index and the SOLERAdrift-search distance to the Sun (green and dark-violet points in central plot), and (3) the directly (SOHO-SEM) measured solar EUV flux rate in [26,34]nm window (bottom plot).

Fig. 3 The EXSOLERAdrift-search result during 9 October 2022 (day 282) is summarized in the top plot vs time: the green dots represent the distance (in degrees) of the direction with the highest significant overionization pattern due to any external source, to GRB221009A, with intensity (in mTECU) represented by the pink crosses. In the bottom plot a vertical zoom is represented.

During this day, when the Sun is considered, we are able to detect in the expected way the weeker flares and sub-flares, like the minor ones (C-class) happened during this day, but not coinciding in time with the GRB221009A occurrence (see Extended Data Figure 4).

Moreover, it can be seen that the 20-units detrended flux peak focused on GRB221009A corresponds to the UT time in seconds of approximately 48010 s practically the starting - growing time of the GRB221009A flux rise following for instance Figure 2 of Pal et al. (2023)[14]. In this work, as it was commented above, a signature of GRB221009A in the Earth ionosphere is reported by means of Very Low and Low Frequency radio signals bouncing at the bottom part of the ionosphere, such as D-layer below 100 km.

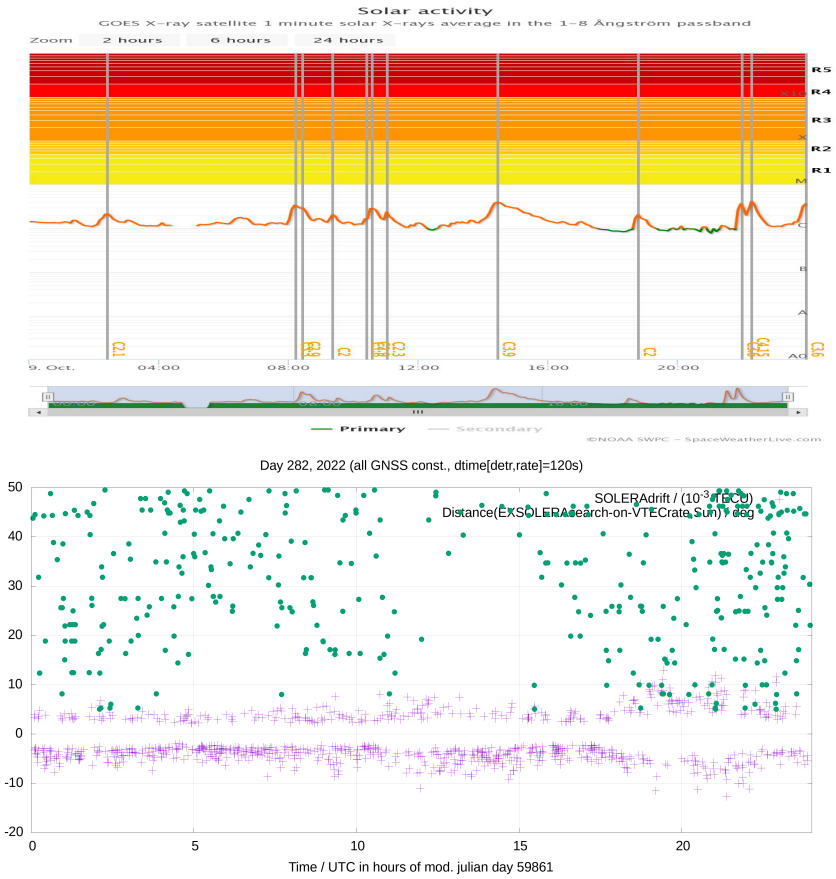

Fig. 4 (Extended Data) Time evolution, during 9 October 2022, day 282, of: (1) the directly (GOES) measured solar flux in X-ray band (1-minute solar average in $[1, 8]\mathring{A}$, top plot), and (2) the indirectly (ionospheric footprint with GNSS) EUV-flux sensitive SOLERAdrift index and the SOLERAdrift-search distance to the Sun (green and dark-violet points in central plot).

And applying EXSOLERAdrift-search at 1s time resolution from the global available network of 1Hz multiGNSS receivers we can see more details (right in Figure **??**), very consistent with direct X-ray and γ-ray measurements provided respectively by Solar Orbiter STIX (counts at 4-10 keV) and Fermi GMB (counts 50-100 keV), as it can be seen in Figure 5. Also in the same figure, we can see in the semi-log plots how the sensitivity to time-shorter increases for instance in X-ray band, is increased when the detrending time is reduced, from 120 s to 60 s (second and third plot of Figure 5), reacting similarly as EXSOLERAdrift-search reacts in front of small variations of X-ray and EUV solar flux (see Figure 2 and corresponding previous comments).

Also, we have redone the study after replacing the ionospheric effective height h_I of 450 km (F2 layer mostly EUV geoeffective, top plot in Figure 6)

Fig. 5 Comparison of 1 Hz GNSS proxies, EXSOLERAdrift (in mTECU, pink crosses) and EXSOLERAdrift-search estimated source distance to GRB221009A (in degrees, green dots), with direct counts provided every 4 seconds, approximately, by Solar Orbiter X-ray STIX detector (4-10 keV, blue triangles) and Fermi GMB counts in γ-ray (yellow triangles), 1000 seconds around the second UTC of the day 48000, i.e. 13h20m UTC 09 October 2022, i.e. the approximate time of GRB221009A event.

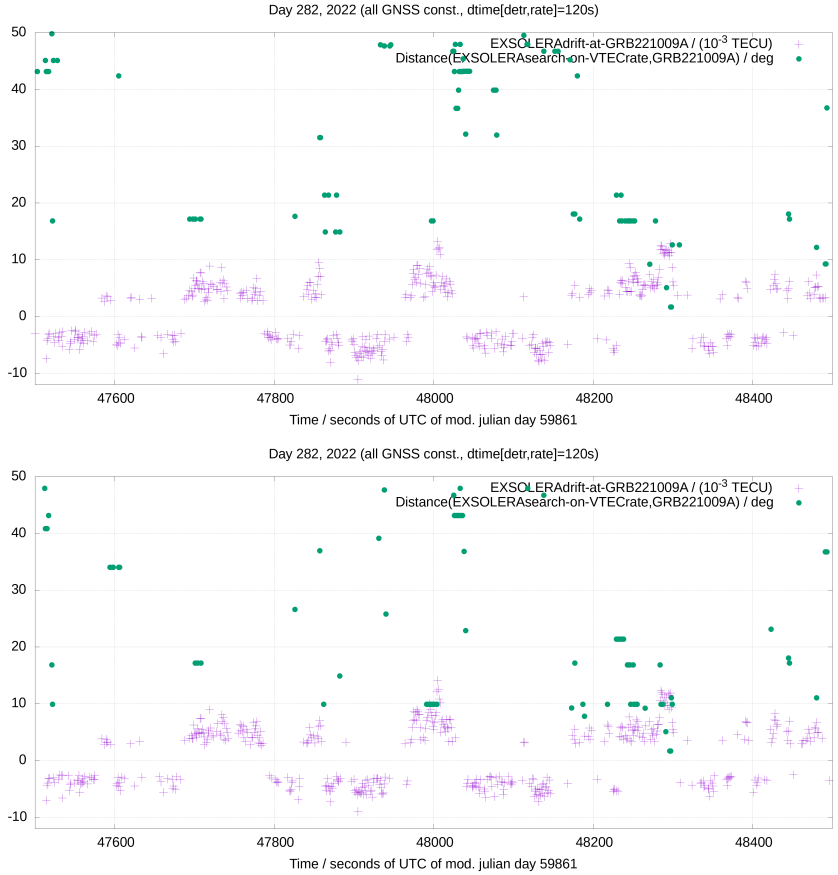

Fig. 6 Comparison of 1 Hz GNSS proxies, EXSOLERAdrift (in mTECU, pink crosses) and EXSOLERAdrift-search estimated source distance to GRB221009A (in degrees, green dots), with ionospheric effective height of 450 km (associated with an important influence of F2 layer, and hence EUV driven overionization of the Earth ionosphere) vs an ionospheric effective height of 75 km (associated to X- and γ-rays driven overionization, bottom plot), 1000 seconds around the second UTC of the day 48000, i.e. 13h20m UTC 09 October 2022, i.e. the approximate time of GRB221009A event.

by 75 km (D layer mostly X-ray geoeffective), which would be in principle the detected perturbed layer by Pal et al. 2023[14], bottom plot in the same figure). At 120 s of detrending time it can be observed an slightly more intense EXSOLERAdrift-search signal under $h_I = 75$ km and an slightly reduced source location error, when it is compared with $h_I = 450$ km. This wwould be compatible with a higher influence of X- (and γ-) rays in the overionization vs EUV flux, that might be more affected by interstellar extinction due to the distance of GRB221009A, similarly as it was demonstrated for the Sun (see Figure 9 in [9]).

In summary, the 24/7 omnidirectional detectability and measurement of very small solar flares and very far huge energetic events like the Gamma

Ray Burst GRB221009A, can be done with a much higher sensitivity than in previous works (e.g. [11]), thanks to a new GNSS Ionosphere based technique, which assess the corresponding overionization pattern, detecting and locating the source.

1 Methods

A solar flare is defined as an extremely high energy explosion on the Sun which generates a burst of electromagnetic waves (from radio waves to EUV-, X- and γ-rays radiation), that occurs when energy stored in twisted magnetic fields (usually above sunspots) is suddenly released.

The solar flares are classified[1] by their X-ray flux in [1,8]Å: major , mid and small (X, M & C-class, see complete definition and description at the introduction).

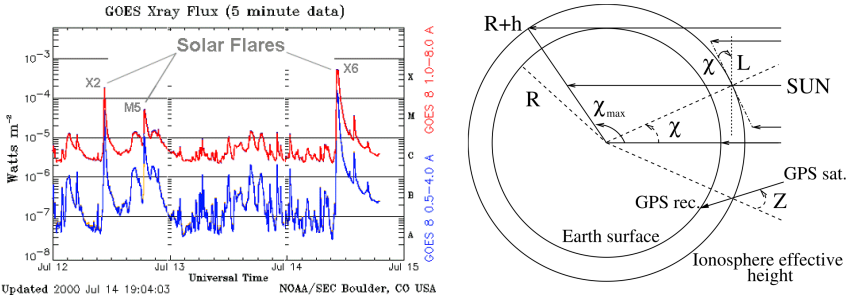

Fig. 7 Left-hand plot: Example of solar X-ray flux measurements from GOES spacecraft during solar flares on July 12-July 14, 2000, extracted from *https://spaceweather.com/glossary/flareclasses.html*; righ-hand plot: layout summarizing the solar flare geoeffectiveness geometry.

1.1 SOLERA model: Method for the estimation of the EUV flux rate

In this section we present a relationship between the variation of electron content in the ionosphere with variations of the EUV flux. This relationship is based on first principles and provides an affine dependence, i.e. of the form $y = ax + b$.

The expected extraordinary rate, of the Vertical Total Electron Content (denoted as V, aka VTEC, see [3]) at the Earth ionosphere due to a solar flare, $\dot{V} \equiv \frac{\partial V}{\partial t}$, for a given solar-zenith angle (or in general, EUV external source - zenith angle) χ corresponding to the Ionospheric Pierce Point (IPP) of the VTEC measurement, can be related with the source solar EUV flux rate, $\dot{I}$, and a projection function C, by means of the geo-effectiveness of the

[1] https://www.esa.int/Science_Exploration/Space_Science/What_are_solar_flares+

considered spectral range, η', following (see Figure 7 and [9]):

$$\dot{V} = \eta' \cdot C(\chi) \cdot \dot{I} \implies \frac{\partial V}{\partial t} = a(t)\cos\chi + b(t) \tag{1}$$

where each GNSS transmitter-receiver ionospheric combination of carrier phases, $L_I = L_1 - L_2$, provide a direct estimation of the VTEC rate as

$$\dot{V} = \frac{1}{M}\frac{dL_I}{dt} \tag{2}$$

being M the ionospheric mapping function at the central time ([3]). And from Equation 1 it is straightforward to see that $a(t)+b(t)$ corresponds to the VTEC rate at sub-solar point mostly due (and proportional by means of physical parameters) to the geoeffective EUV flux rate associated to the flare [11]. This can be computed in the source-illuminated ionosphere after estimating at each given time t two global unknowns, a and b by Least Squares with removal of outliers[2] on the available observational pairs $\{(\chi_j, \dot{V}_j)\}_{j=1,N_{obs}}$, directly measured at several ionospheric (i.e. geometry-free) combinations of GNSS carrier phases from typically +100 ground GNSS receivers and +10 GNSS transmitters at each second (high-rate), or at 30 seconds. This brings, for example, on disposing of a set of $N_{obs} \simeq 5 \cdot 10^8$ worldwide observations (high-rate) during the first analyzed day, 142 of year 2021, when multi-GNSS measurements of +200 worldwide receivers were available. The expected normalized increase of VTEC in the ionosphere is represented in left hand plot of Figure 8, following Equation 3 (the source is indicated by a cross).

Other way of solving Equation 1 consists on estimating only the unknown α after assuming that

$$\dot{V} \simeq \alpha \cdot \frac{\cos\chi + 0.2}{1 + 0.2} \tag{3}$$

where $b \simeq 0.2 \cdot a$, and $\alpha = a(1 + 0.2)$ is the sub-source flux rate, directly estimated in this approximation as a single unknown per time. This empirical relationship (see for instance Figure 1 at [11]) is associated to the typical effective height of few hundreds of km at which the over-ionization occurs. Under the SOLar Euv flux RAte GNSS proxy (SOLERA) term we will refer to any of these direct estimations $a(t) + b(t)$ or $a(t)$, and under any of both, one- or two- unknown per epoch, models. And we will use the term EXtra SOLar sources search based on EUV, X-ray or γ-ray radiation RAte from GNSS (EXSOLERA) when we refer to extra-solar sources of EUV (or X-ray and γ-ray) variations beyond the Sun.

Last but not least, in order to focus on the demanding detection of significant EUV flux increase from any source far from the Earth, we will consider

[2]Note that the method for removing outliers, was proposed in [9], which is related to the RANdom SAmple Consensus (RANSAC) method used in machine learning [15], but the method proposed in [9] is more robust to long tail outliers.

the fast detrended VTEC at different time scales δt,

$$\tilde{V}(t) = V(t) - \frac{V(t-\delta t) + V(t+\delta t)}{2} \tag{4}$$

(formally related with the drift rate, $\ddot{V} = -2\tilde{V}/\delta t$) by applying correspondingly the (EX)SOLERA model:

$$\tilde{V} = \eta' \cdot C(\chi) \cdot \tilde{I} \implies \tilde{V} = \tilde{a}(t)\cos\chi + \tilde{b}(t) \tag{5}$$

We use the name of (EX)SOLERAdrift for the model summarized in Equation 5.

1.2 (EX)SOLERAdrift-search model

In order to increase the reliability of the potential detection of small EUV flux increase events, from the Sun and from potential extrasolar sources, we introduce the (EX)SOLERAdrift-search model which allows to estimate as well the position of the potential source, alternatively to previous approaches [12].

Indeed it consists on estimating the fitting parameters from $\tilde{V}$, for each one of the potential source positions defined in a global grid (e.g. with separations of 10° and 5° in right ascension and declination in this work), like the one represented at the right-hand plot of Figure 8, and selecting the one providing the highest Pearson correlation coefficient after solving the linear model given in Equation 5. And at the same time we will compute the corresponding model indices estimated in such equations pointing directly the active source for which we dispose of independent direct flux measurements (the Sun and GRB221009A in this work). We will focus on those fulfilling a p-value of the null hypothesis below 5%, by assuming a joint probability distribution of both correlated variables x and y not too different from a binormal distribution (see for instance pages 632 and 633 in [16]). And we will monitor at the same time the distance over the celestial sphere of the estimated (EX)SOLERAdrift-search source position (the one with highest Pearson correlation coefficient among the global grid of potential sources) vs the active source for which we dispose of such direct independent flux measurements.

2 Data availability

The GNSS data collected by the International GNSS Service, used in this study, can be openly obtained at http://cddis.gsfc.nasa.gov after soliciting the free open access. The GOES X-ray plots have been generated thanks to SpaceWeatherLive.com facility (https://www.spaceweatherlive.com/en/archive/.html); And the Solar Heliospheric Observatory (SOHO) Solar EUV Monitor (SEM) measurements can be downloaded from https://lasp.colorado.edu/eve/data_access/eve_data/lasp_soho_sem_data/long/15_sec_avg.

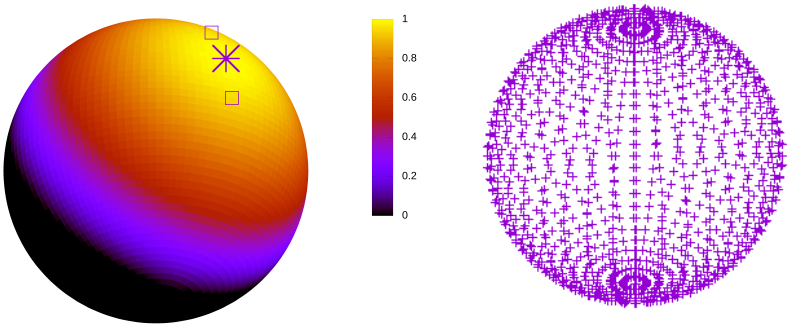

Fig. 8 Left-hand plot: Expected footprint over the Earth ionosphere of an increase of an external source EUV flux, normalized to one at the sub-source point (Equation 3), represented by a cross (the squares represent two points at a distance of 20° in the same celestial equatorial meridian); right-hand plot: example of distribution of potential external EUV sources considered in the (EX)SOLERAdrift-search technique (10° in right ascension and 5° in declination, among potential source at every pole).

Acknowledgments. This work has been performed under the GNSS-Astronomy project, under ESA Contract No. 4000133257/20/NL/GLC with UPC, and it has been developed coinciding with the PITHIA-NRF European project (H2020-INFRAIA-2018-2020101007599).

Author contributions. M.H.P. was the principal investigator of the GNSS Astronomy project, and the associated research summarized in this manuscript. D.M.B. contributed running the previous technique for comparison. O.F. provided astronomical inputs and support to this work. J.P. gathered and adapted the Solar Orbiter X-ray and Fermi γ-ray reference measurements for the study of the GRB221009A event. Q.L. identified the target day for the study of the solar sub-flares and the SOHO-SEM EUV measurements. J.V.T. and R.O.P. funded the research. M.H.P., D.M.B., O.F., J.P., Q.L., V.G., G.O.P., D.R.D., A.G.R., E.M.M., H.Y., H.L., J.M.G.C., J.V.T. and R.O.P. shared ideas, interpreted the results, commented and edited the manuscript.

References

[1] Hernández-Pajares, M.: Gnss ionosphere. Encyclopedia of Geodesy, 1–7 (2022)

[2] Hernández-Pajares, M., Juan, J., Sanz, J., Orus, R., García-Rigo, A., Feltens, J., Komjathy, A., Schaer, S., Krankowski, A.: The IGS VTEC maps: a reliable source of ionospheric information since 1998. Journal of Geodesy **83**(3-4), 263–275 (2009)

[3] Hernández-Pajares, M., Juan, J.M., Sanz, J., Aragón-Àngel, À., García-Rigo, A., Salazar, D., Escudero, M.: The ionosphere: effects, GPS modeling and the benefits for space geodetic techniques. Journal of Geodesy **85**(12), 887–907 (2011). https://doi.org/10.1007/s00190-011-0508-5

[4] Liu, Q., Hernández-Pajares, M., Yang, H., Monte-Moreno, E., Roma-Dollase, D., García-Rigo, A., Li, Z., Wang, N., Laurichesse, D., Blot, A., *et al.*: The cooperative igs rt-gims: a reliable estimation of the global ionospheric electron content distribution in real time. Earth System Science Data **13**(9), 4567–4582 (2021)

[5] Hernández-Pajares, M., Juan, J., Sanz, J., Colombo, O.L.: Application of ionospheric tomography to real-time GPS carrier-phase ambiguities Resolution, at scales of 400–1000 km and with high geomagnetic activity. Geophysical Research Letters **27**(13), 2009–2012 (2000)

[6] Hernández-Pajares, M., Olivares-Pulido, G., Graffigna, V., García-Rigo, A., Lyu, H., Roma-Dollase, D., de Lacy, M.C., Fernández-Prades, C., Arribas, J., Majoral, M., *et al.*: Wide-area gnss corrections for precise positioning and navigation in agriculture. Remote Sensing **14**(16), 3845 (2022)

[7] Hernández-Pajares, M., Juan, J.M., Sanz, J., Colombo, O.L., van der Marel, H.: A new strategy for real-time integrated water vapor determination in wadgps networks. Geophysical Research Letters **28**(17), 3267–3270 (2001)

[8] Yang, H., Hernández-Pajares, M., Jarmołowski, W., Wielgosz, P., Vadas, S.L., Colombo, O.L., Monte-Moreno, E., Garcia-Rigo, A., Graffigna, V., Krypiak-Gregorczyk, A., *et al.*: Systematic detection of anomalous ionospheric perturbations above leos from gnss pod data including possible tsunami signatures. IEEE Transactions on Geoscience and Remote Sensing **60**, 1–23 (2022)

[9] Hernández-Pajares, M., García-Rigo, A., Juan, J.M., Sanz, J., Monte, E., Aragón-Àngel, A.: Gnss measurement of euv photons flux rate during strong and mid solar flares. Space Weather **10**(12) (2012). https://doi.org/10.1029/2012SW000826

[10] Monte-Moreno, E., Hernández-Pajares, M.: Occurrence of solar flares viewed with gps: Statistics and fractal nature. Journal of Geophysical Research: Space Physics **119**(11), 9216–9227 (2014)

[11] Singh, T., Hernandez-Pajares, M., Monte, E., Garcia-Rigo, A., Olivares-Pulido, G.: Gps as a solar observational instrument: Real-time estimation of euv photons flux rate during strong, medium, and weak solar flares. Journal of Geophysical Research: Space Physics **120**(12) (2015). https:

//doi.org/10.1002/2015JA021824

[12] Hernández-Pajares, M., Moreno-Borràs, D.: Real-time detection, location, and measurement of geoeffective stellar flares from global navigation satellite system data: New technique and case studies. Space Weather **18**(3), 2020–002441 (2020)

[13] Gehrels, N., Mészáros, P.: Gamma-ray bursts. Science **337**(6097), 932–936 (2012)

[14] Pal, S., Hobara, Y., Shvets, A., Schnoor, P.W., Hayakawa, M., Koloskov, O.: First detection of global ionospheric disturbances associated with the most powerful gamma ray burst grb221009a. Atmosphere **14**(2), 217 (2023)

[15] Cantzler, H.: Random sample consensus (ransac). Institute for Perception, Action and Behaviour, Division of Informatics, University of Edinburgh (1981)

[16] Press, W.H., Flannery, B.P., Teukolsky, S.A., Vetterling, W.T., et al.: Numerical recipes. Cambridge university press Cambridge (1989)